Z. Phys. C – Particles and Fields 45, 1–10 (1989)

Zeitschrift für Physik C Particles and Fields

Comparison of inclusive fractional momentum distributions of quark and gluon jets produced in e^+e^- annihilation

TASSO Collaboration

W. Braunschweig, R. Gerhards, F.J. Kirschfink, H.-U. Martyn

I. Physikalisches Institut der RWTH, Aachen, Federal Republic of Germany[a]

B. Bock[1], H.M. Fischer, H. Hartmann, J. Hartmann, E. Hilger, A. Jocksch, R. Wedemeyer

Physikalisches Institut der Universität, Bonn, Federal Republic of Germany[a]

B. Foster, A.J. Martin

H.H. Wills Physics Laboratory, University of Bristol, Bristol, UK[b]

E. Bernardi[2], J. Chwastowski[3], A. Eskreys[3], K. Gather, K. Genser[4], H. Hultschig, P. Joos, H. Kowalski, A. Ladage, B. Löhr, D. Lüke, P. Mättig[5], D. Notz, J.M. Pawlak[4], K.-U. Pösnecker, E. Ros, D. Trines, R. Walczak[4], G. Wolf

Deutsches Elektronen-Synchrotron DESY, Hamburg, Federal Republic of Germany

H. Kolanoski

Institut für Physik, Universität, Dortmund, Federal Republic of Germany[a]

T. Kracht[6], J. Krüger, E. Lohrmann, G. Poelz, W. Zeuner[7]

II. Institut für Experimentalphysik der Universität, Hamburg, Federal Republic of Germany[a]

J. Hassard, J. Shulman, D. Su[8], I.R. Tomalin

Department of Physics, Imperial College, London, UK[b]

F. Barreiro, A. Leites, J. del Peso

Universidad Autonoma de Madrid, Madrid, Spain[c]

M.G. Bowler, P.N. Burrows[9], R.J. Cashmore, G.P. Heath, M.E. Veitch

Dept. of Nuclear Physics, Oxford University, Oxford, UK[b]

J.C. Hart, D.H. Saxon

Rutherford Appleton Laboratory, Chilton, Didcot, UK[b]

S. Brandt, M. Holder

Fachbereich Physik der Universität-Gesamtschule, Siegen, Federal Republic of Germany[a]

Y. Eisenberg[10], U. Karshon, G. Mikenberg, A. Montag, D. Revel, E. Ronat, A. Shapira, N. Wainer, G. Yekutieli

Weizmann Institute, Rehovot, Israel[d]

D. Muller, S. Ritz[11], D. Strom[12], M. Takashima, Sau Lan Wu, G. Zobernig

Department of Physics, University of Wisconsin, Madison, WI, USA[e]

Received 22 May 1989

[1] Now at Krupp Atlas Elektr. GmbH, Bremen, FRG
[2] Now at Robert Bosch GmbH, Schwieberdingen, FRG
[3] Not at Inst. of Nuclear Physics, Cracow, Poland
[4] Now at Warsaw University[f], Poland
[5] Now at IPP Canada, Carleton University, Ottowa, Canada
[6] Now at Hasylab, DESY
[7] Now at CERN, Geneva, Switzerland
[8] Now at RAL, Chilton, Didcot, UK
[9] Now at MIT, Cambridge, MA, USA
[10] The Nicki and J. Ira Harris professorial chair
[11] Now at Columbia University, NY, USA
[12] Now at University of Chicago, Chicago, IL, USA

[a] Supported by Bundesministerium für Forschung und Technologie
[b] Supported by UK Science and Engineering Research Council
[c] Supported by CAICYT
[d] Supported by the Minerva Gesellschaft für Forschung GmbH
[e] Supported by US Dept. of Energy, contract DE-AC02-76ER000881 and by US Nat. Sci. Foundation Grant no INT-8313994 for travel
[f] Partially supported by grant CPBP 01.06

Abstract. Inclusive charged particle production in e^+e^- annihilation into hadrons is studied in terms of the particle fractional momentum x_p. The x_p distribution for gluon jets is extracted by comparing two data samples measured in the TASSO detector: nearly symmetric three jet events at centre-of-mass energy $W\sim 35$ GeV and two jet events at $W\sim 22$ GeV, yielding quark and gluon jets of similar energies (~ 11.5 GeV). No significant difference is observed between quark and gluon jets. Monte Carlo models based on parton showers describe the trend and energy variation of the data better than a model with second order matrix element in α_s.

1 Introduction

Quantum chromodynamics (QCD) is able to describe quantitatively strong interactions at high Q^2, where perturbative calculations are valid. At low Q^2 the quarks and gluons are confined by the colour field, so that only colour-singlet hadrons are observed. These hadrons are collimated into jets whenever the initial partons are energetic enough.

Large amounts of data exist on fragmentation of quark and antiquark jets. However little is known experimentally on fragmentation of high energy gluon jets. QCD predicts larger multiplicity and consequently softer fragmentation for gluon jets compared to quark jets of the same energy. The ratio r between gluon jet multiplicity and quark jet multiplicity is predicted [1] to be $r=9/4$ at the limit of infinite energy. This ratio is calculated in QCD for parton multiplicities. Assuming [1, 2] that parton and hadron multiplicities are related through a phenomenological energy independent parameter, this ratio should also be valid for hadron multiplicities. Finite energy corrections up to second order in α_s yield [3] a value of $r\sim 2$. Adding heavy quark effects [2] further reduces the value of r. The formalism developed in reference [2] was applied to estimate r for the kinetmatical conditions of the present work, yielding $r\sim 1.3$.

Most of the experimental data on gluon jet fragmentation come from $e^+e^-\to q\bar{q}g$. High energy e^+e^- collisions are ideal for such studies because of the simplicity of the parton level process. However most studies of gluon jet fragmentation in e^+e^- annihilation have led to inconclusive results. The HRS Collaboration [4] has studied the multiplicity distribution of charged particles in gluon jets in symmetric three jet events. They compared gluon jets to quark jets in the same events obtaining $\frac{n_g}{n_q}=1.25^{+0.17}_{-0.32}\pm 0.20$ for the ratio of gluon jet multiplicity to quark jet multiplicity. The MARK II Collaboration [5] has studied inclusive charged particle distributions in terms of the fractional momentum $x_p=\frac{p_i}{E_j}$, where p_i is the momentum of the charged particle i and E_j is the energy of the jet to which it is assigned. Their study apparently favours a softer gluon fragmentation. The JADE Collaboration [6] has reported that particles coming from the least energetic jet (the most probable to be a gluon jet) in three jet events tend to carry on the average larger p_t. They report $\frac{\langle p_{t3}\rangle}{\langle p_{t2}\rangle}=1.16\pm 0.02$ where jet 3 is the least energetic one and jet 2 is the next in energy. Other, preliminary, results are less striking. The TPC Collaboration [7] reports $\frac{\langle p_{t3}\rangle}{\langle p_{t2}\rangle}=1.08\pm 0.02$. The CELLO Collaboration [8] compared the least energetic jet in three jet events at c.m. energy $W=35$ GeV to two jet events at $W=14$ GeV, thus comparing a gluon enriched sample of jets to a quark enriched sample. They report $\frac{\langle p_{t3}(35)\rangle}{\langle p_t(14)\rangle}=1.03\pm 0.03\pm 0.04$, not seeing an increase in p_t for gluon jets.

In $p\bar{p}$ collisions at the CERN $Sp\bar{p}S$, gluon jets are more energetic and predominate in the region of low transverse momentum. The UA1 Collaboration [9] studied jet fragmentation in $p\bar{p}$ collisions. Comparison of charged multiplicity between quark and gluon jets could not be done due to systematic uncertainties in the charge multiplicity of the quark jet sample. However, they were able to show that pairs of gluon jets with invariant mass of 95 GeV fragment more softly than pairs of quark jets at invariant mass of 130 GeV. Note that the mean transverse momenta with respect to the beam axis for the two types of jets are similar, 35 GeV and 39 GeV respectively.

In this paper we study inclusive charged particle production in nearly symmetric three jet events produced in e^+e^- annihilation. We assume that these events consist of two quark jets and one gluon jet. The inclusive charged particle distribution is studied in terms of the fractional momentum x_p. In order to avoid scale breaking effects it is necessary to compare charged particle production in quark and gluon jets of the same energy. PETRA has provided us with data at c.m. energies of $W\sim 35$ GeV and $W\sim 22$ GeV. Therefore, we can compare the x_p distribution of charged particles in the high energy events with three jets ($q\bar{q}g$) each of ~ 11.6 GeV energy to the same distribution in jets of ~ 11.2 GeV energy in two jet ($q\bar{q}$) events at the lower energy. In this comparison the gluon jet distribution can be extracted without assum-

ing that the least energetic jet is most probably the gluon jet.

Although it has been shown that the jets do not fragment independently, misassignment of a particle to its jet is not crucial for the x_p measurement, as the energies of the three jets are almost equal. The jet axes are used only in the event selection (see below) and in the jet energy determination, thus the dependence of the results on the jet finding algorithm is minimal. Studies of quantities like jet particle multiplicity, rapidity, or p_t with respect to jet axes, are much more dependent on the reconstructed jet directions. With this procedure we keep systematic errors at a minimum by comparing data taken by the same detector at two different c.m. energies.

2 Data selection and corrections

2.1 General

The data were taken with the TASSO detector at PETRA at two regions of centre-of-mass energies: $30<W<38$ GeV, with an average of $\bar{W}=34.8$ GeV, and $22<W<25$ GeV, with $\bar{W}=22.3$ GeV. The corresponding integrated luminosities were 190 pb^{-1} and 3.2 pb^{-1} respectively. Details of the detector can be found elsewhere [10].

The selection of multihadronic final states from e^+e^- annihilation was based upon charged particles measured in the central detector. The selection criteria, as described in detail in [11], yield 53559 events at $\bar{W}=34.8$ GeV and 2145 events at $\bar{W}=22.3$ GeV. The main requirements are: a charged track is accepted if its momentum transverse to the beam direction is $p_{xy}>0.1$ GeV/c and its polar angle satisfies $|\cos\theta|<0.87$; the momentum sum of all accepted charged particles has to be in the range $0.265\ W<\Sigma p_i<2\ W$. The r.m.s. track momentum resolution, including multiple scattering, is $\sigma_p/p=0.016(1+p^2)^{1/2}$, with p in GeV/c. The contamination to the single photon (or Z_0) hadronic data sample from other processes within the accepted events was estimated by Monte Carlo simulation and found to be very small [11, 12]: negligible for beam-gas interactions, 0.9% (0.6%) for $\gamma\gamma$ scattering and 0.8% (1.1%) for τ pair production at $\bar{W}=34.8$ GeV ($\bar{W}=22.3$ GeV).

In order to reject events with badly reconstructed tracks and events with a hard photon radiated from the incoming e^+ or e^-, two additional cuts are made: (a) the angle θ_s between the sphericity axis and the beam direction is required to satisfy $|\cos\theta_s|<0.85$; (b) the angle θ_N between the normal to the event plane and the beam direction has to satisfy $|\cos\theta_N|>0.1$. The number of multihadronic events remaining after these cuts are 45852 for $\bar{W}=34.8$ GeV and 1948 for $\bar{W}=22.3$ GeV.

2.2 Three jet events

Our selection method consists of finding 3-jet events at c.m. energy $W\sim35$ GeV with the 3 jets having nearly the same energy, to be compared with two jet events of the same jet energy. Assuming the 3-jet events originate from $q\bar{q}g$, the gluon fragmentation can be extracted.

For the comparison to be meaningful, it is necessary to use a reliable jet finding algorithm. Four different algorithms have been checked, using the LUND Monte Carlo [13] with a second order matrix element in α_s. All the Monte Carlo events, with initial state radiative effects included, were processed through a detailed TASSO detector simulation program [14], and were subjected to the same hadronic selection criteria. Three jet analysis cuts were then applied as in the data. One algorithm [15] was discarded because it gave too many multijet events. We have also tested an algorithm [16] based on a mass cut on the invariant mass between any pair of jets, an algorithm [13] based on a similar mass cut weighted by the particle momenta, and an algorithm [17] based on the sphericity tensor. The selection of the best algorithm was based mainly on the goodness of reconstruction of the least energetic jet in a symmetric three jet event as given by, among other quantities, the angle between the direction of the reconstructed jet and the direction of the original parton, and the reconstructed energy (as given by the angles between jets, see below). The results are shown in Table 1.

The main background to our sample are events with more than three jets. Therefore, another important factor to consider in choosing the best algorithm, is the contamination from four jet events. As the cross sections for 3 and 4 parton events in second order QCD become infinite for soft gluon production, cutoffs have to be applied in order to remove the infrared and collinear singularities. Two methods are often used for this purpose. The first one is the Sterman-Weinberg [18] definition of a jet, which requires minimal values for the fractional energy $\varepsilon_j=2\frac{E_j^{\text{parton}}}{W}$ of each parton j and for the angle δ_{ij} between any pair of partons i and j. The second method is the one used by the GKS [19] calculation of second order α_s matrix elements. These matrix elements are incorporated in the LUND Monte Carlo, and the singularities on them are removed by requiring a lower limit to the variable $y_{ij}^{\text{parton}}=\frac{(p_i+p_j)^2}{W^2}$, where p_i and p_j are

Table 1. Comparison of different jet finding algorithms using the LUND Monte Carlo with second order matrix element in α_s. Jet 3 is the least energetic jet

Selected algorithm	Gen. sphe. Ref. [17]		W. inv. mass Ref. [13]		Inv. mass Ref. [16]	
	Mean	RMS	Mean	RMS	Mean	RMS
Angle between reconstructed and generated jet for jet 3	17.5°	26.1°	20.0°	26.0°	19.1°	24.8°
Scaled generated energy of jet 3	0.54	0.13	0.56	0.16	0.57	0.15
Difference between generated and reconstructed scaled energies for jet 3	−0.04	0.12	−0.06	0.13	−0.07	0.13
Contamination of 4 jet events $\delta_{ij}>55°$, $\varepsilon_j>0.24$		10%		12%		14%
Contamination of 4 jet events $y_{ij}^{\text{parton}}>0.04$		8%		10%		11%

the 4-momenta of any 2 partons. The cutoff used in the LUND Monte Carlo is $y_{\min}=0.02$. The 4-jet contamination for the different jet algorithms has been estimated by counting the number of 4-parton events in a symmetric 3-jet Monte Carlo sample that passed appropriate cutoffs for both methods. The results are given in Table 1.

Based on the overall results for the various algorithms, summarized in Table 1, we decided to use the generalized sphericity method [17] to select symmetric three jet events. A brief description of the method follows.

As 3-jet events are planar, this algorithm projects all particle momenta into the event plane, which is defined by the two eigenvectors of the sphericity tensor that correspond to the two largest eigenvalues. To find the jet axes, all the particles are divided into three non-overlapping sets that minimize the sum of reduced sphericities:

$$\sum_{j=1}^{3} S'_j = \sum_{j=1}^{3} \frac{\Sigma_i p_{i\perp}^2}{\Sigma_i p_i^2}$$

where i runs over all particles of jet j, p_i is the momentum of particle i projected into the event plane and $p_{i\perp}$ is its component in this plane transverse to the axis of jet j.

The method described above assigns three jet axes for every event. We apply a set of energy-angle cuts to select a sample of symmetric three jet events. This is done in two steps. The first one is an optimized set of cuts to define 3-jet events which, as given in [20], are:

- For each jet, $x_{\text{vis}}>0.12$, where $x_{\text{vis}}=\dfrac{E_{\text{jet}}}{E_{\text{beam}}}$, and E_{jet} is the total energy of all measured charged particles in the jet, assumed to be pions. The number of events passing this cut is 28987.
- $\phi_i>55°$, where ϕ_i is the angle between any 2 jets j and k, and i, j and k are cyclic. The number of events surviving this cut is 9658.
- The 3 jets are not in the same half of the event plane. This requirement leaves 8497 events.
- For each jet, $x_{\text{cal}}>0.24$ where x_{cal} is given by the following expression which assumes massless partons:

$$x_{\text{cal},i}=\frac{2\sin\phi_i}{\sum_{j=1}^{3}\sin\phi_j}=\frac{E_{\text{cal},i}}{E_{\text{beam}}}; \quad \left(\sum_{i=1}^{3} x_{\text{cal},i}=2\right).$$

A total of 5830 events survived all the above cuts.

In the second step, additional cuts are applied in order to select a symmetric 3-jet sample:

- $100°<\phi_i<140°$. This cut reduces the sample to 559 events.
- Defining an observed jet as the vector sum of the 3-momenta of all charged particles belonging to a given reconstructed jet, we require $350°<\sum_{i=1}^{3}\psi_i<370°$, where the ψ_i's are the angles between any pair of observed jets. After this cut 521 events remained.
- $A_{\text{pl}}<0.1$ where A_{pl} is the aplanarity of the event. This cut and the previous one are imposed to diminish background from multijet events. 427 events survived this cut.
- Each event from the above data sample was visually scanned. One event was discarded due to the fact that the third jet apparently originated from a converted photon.
- At least 2 charged particles were required to define a jet. This cut removes spurious jets leaving a final sample of 396 events.

Monte Carlo studies showed that this sample has no background of 2-jet events, τ pairs or $\gamma\gamma$ events. The only source of background is 4-jet events. The treatment of this type of background is such that on one hand we try to minimize it, for example by applying $\sum\psi_i$ and A_{pl} cuts as above. On the other hand, a contamination of an $(n+1)$-jet configuration within an n-jet sample tends to soften the x_p distribution

of this sample. Therefore, it is preferable to have similar values for the fraction of 4-jet events in the 3-jet sample and for the fraction of 3-jet events in the 2-jet sample. This will ensure a meaningful comparison between the x_p distributions of the 3-jet and 2-jet samples.

Previous analyses of multijet final states have demonstrated [16, 21] that Monte Carlo QCD models with a second order matrix element in α_s yield 4-jet rates which are too low compared with the observed 4-jet events. Recently, it has been shown that the 4-jet rate can be enhanced by optimizing the renormalization scale [22]. QCD models with a parton shower before fragmentation describe satisfactorily the multi-parton rates and have been tuned to the global features of our data. The 4-jet contamination in our symmetric 3-jet sample has been estimated with the LUND 6.3 Monte Carlo program [13] with the parton shower option.

Since it is not easy to relate partons to hadronic jets in such a model, the JADE cluster algorithm [16] was directly applied to the partons before hadronization, as well as to the hadrons of the simulated events and of the data. As was shown in [16, 21] the fraction of 4-jet events is a decreasing function of the jet resolution parameter y_c, which is a lower limit to the variable $y_{ij}=2\,E_i\,E_j\dfrac{(1-\cos\theta_{ij})}{E_{\text{tot}}^2}$, where y_{ij} is calculated for all pairs of partons or charged hadrons i,j (assumed to be pions) in an event. E_{tot} is the total visible energy for charged hadrons in an event or the total c.m. energy for partons after initial state photon radiation. The above y_{ij} definitions were found [16, 21] to provide the best agreement between hadron and parton cluster multiplicities in the multihadronic sample for reasonable values of y_c.

The fractions of 3- and 4-clusters in the symmetric 3-jet events are shown in Fig. 1 as a function of y_c for the data (points) and for the simulated events which passed all the cuts of the symmetric 3-jet sample (solid curves). The QCD model and the data are in good agreement. The 3- and 4-parton cluster fractions are also shown as a function of y_c (dashed curves). Both the 3- and 4-jet rates at the parton and hadron levels are similar for all y_c values shown. For low y_c values ($\leqq 0.06$), fluctuations due to the fragmentation process dominate the reconstruction of clusters [16, 21]. A safe upper limit for the 4-jet contamination in the symmetric 3-jet sample, taking the 4-parton cluster fraction at $y_c=0.06$, is 5%.

2.3 Two jet events

In this paper, all events of the $\bar{W}=22.3$ GeV data sample, described in Sect. 2.1, are regarded as 2-jet events, where each jet has an energy of ~ 11.2 GeV.

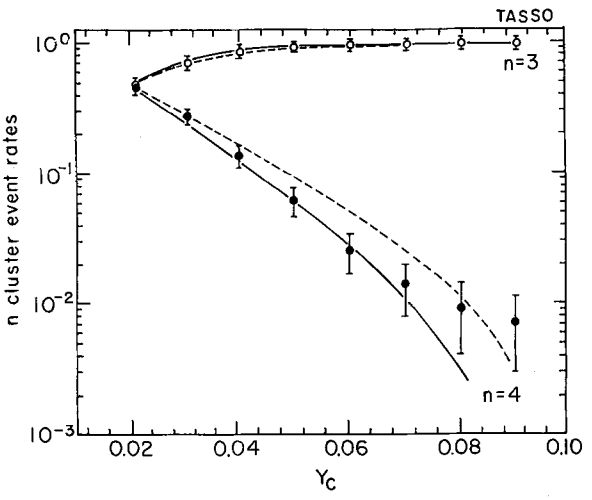

Fig. 1. The fractions of 3- and 4-clusters in the symmetric 3-jet events as a function of the jet resolution parameter y_c for the data (points) and for Monte Carlo events (curves) generated with the LUND 6.3 program with the parton shower option. The solid line shows the simulated hadrons after detector simulation and selection criteria and the dashed line represents the partons in the above generated events

In Sect. 2.2 it was stated that the desired situation is to have a 3-jet contamination in the 2-jet sample similar to the 4-jet contamination in the symmetric 3-jet sample. The latter fraction has been estimated in the previous section to be less than 5%. Applying the energy-angle cuts as described in Sect. 2.2 on the $\bar{W}\sim 22$ GeV data sample, by scaling up the x_{vis} and x_{cal} cuts such that the E_{jet} and $E_{\text{cal},i}$ cuts are left unchanged, we obtain a contamination of $\sim$4–5% of 3-jet events in the 2-jet sample. Therefore, we have preferred not to remove the 3-jet events from the 22 GeV sample.

A multiplicity cut has also been imposed on the 2-jet event sample. Each event was divided into two hemispheres, defined by a plane perpendicular to the event sphericity axis. At least 2 charged particles were required to be in each hemisphere. This cut, which is analogous to the jet multiplicity cut of the 3-jet sample (Sect. 2.2), yields a final 2-jet sample of 1828 events at $\bar{W}=22.3$ GeV. Monte Carlo studies showed [12] that the contamination of $\gamma\gamma$ and τ-pair events in this sample is even smaller than the numbers of Sect. 2.1.

2.4 Corrections

The distributions presented below have been corrected for acceptance, detector efficiency, initial state radiation and the selection cuts described in Sect. 2.1, using the LUND 6.3 Monte Carlo simulation [13]. Initially, N_{gen}^{22} events were generated at $W=22$ GeV, with no QED radiative corrections. Events at

$\bar{W}=35$ GeV were generated without raditive corrections and passed through the 3-jet cuts described in Sect. 2.2 to yield N_{gen}^{35} events. These events yielded the x_p distributions $n_{\text{gen}}^{W}(x_p)$ of charged particles which were produced either in the fragmentation process or from the decay of particles with lifetimes of less then 3×10^{-10} s. A second set of events was then generated for both energies, including QED radiative effects, and traced through a simulation of the TASSO detector, thereby producing hits in the tracking chambers. Energy loss, multiple scattering, photon conversion and nuclear interactions in the material of the detector as well as decays were taken into account. The events were then passed through the track reconstruction, acceptance and analysis programs used on the real data, yielding N_{det}^{W} accepted events corresponding to the x_p distributions $n_{\text{det}}^{W}(x_p)$. The fraction of symmetric 3-jet events that survived all the cuts was found to be similar to that in the data. The correction factors $C^{W}(x_p)$ for every bin and for both energies are calculated as:

$$C^{W}(x_p)=\frac{n_{\text{det}}^{W}(x_p)}{N_{\text{det}}^{W}}\cdot\left(\frac{n_{\text{gen}}^{W}(x_p)}{N_{\text{gen}}^{W}}\right)^{-1}.$$

The corrected distribution $n_{\text{corr}}^{W}(x_p)$ is then derived from the measured distribution $n_{\text{meas}}^{W}(x_p)$:

$$n_{\text{corr}}^{W}(x_p)=\frac{n_{\text{meas}}^{W}(x_p)}{C^{W}(x_p)}.$$

These correction factors $C^{W}(x_p)$ lie in the range $0.8<C^{W}(x_p)<0.9$ up to $x_p=0.6$ and rise smoothly up to $C^{W}(x_p)=1.4$ for the highest x_p value used. The reason for the rise in the correction factor for particles with large momentum is that the error in the momentum measurement is proportional to the square of the momentum of the particle. Therefore the error in x_p for these particles can reach 10% or more, so that particles with lower momentum can be wrongly measured, giving more entries in the highest bin.

We calculated the correction factors with the LUND 6.3 Monte Carlo program [13], using two different options: the matrix element option with second order in α_s, and the parton shower option. The difference in the values of the correction factors between the two generators was taken as the systematic error. Other effects, as discussed for example in [11], are negligible. It is typically below 5% for $x_p<0.5$, on the order of 10% for $0.5<x_p<0.7$ and on the order of 20% for $0.7<x_p<0.8$.

3 Results

The corrected x_p distribution originating from events containing two quark jets and one gluon jet, each with approximately 11 GeV energy, is compared with the corrected x_p distribution originating from events containing two quark jets of the same energy. In order to extract the x_p distribution of a gluon jet with the same energy, the following relation was used:

$$\frac{1}{\sigma_3^{\text{tot}}}\frac{d\sigma}{dx_p}(\text{gluon jets})=\frac{1}{\sigma_3^{\text{tot}}}\frac{d\sigma}{dx_p}(\text{3-jets})-\frac{1}{\sigma_2^{\text{tot}}}\frac{d\sigma}{dx_p}(\text{2-jets})$$

where "3 jets" are the symmetric three jet events at c.m. energy of 35 GeV, "2 jets" are all the events at c.m. energy of 22 GeV, and $\sigma_3^{\text{tot}}(\sigma_2^{\text{tot}})$ is the total cross section for our 3-jet (2-jet) sample.

The x_p distributions of the two data samples and of the "gluon jets" are presented in Table 2. The 3-jet and the 2-jet distributions are similar, yielding also a similar gluon jet x_p distribution. The trend of the data can be seen in Fig. 2.

Table 2. $d\sigma/dx_p$ distributions of 2-jet, 3-jet and extracted gluon jet data, divided into 0.1 bins and normalized as in Fig. 2. The first error is statistical and the second is systematic

x_p	2-jet	3-jet	gluon jet
0.05	$37.25\pm0.37\pm0.96$	$37.23\pm0.68\pm0.58$	$37.19\pm1.29\pm0.96$
0.15	$12.44\pm0.22\pm0.45$	$12.34\pm0.40\pm0.17$	$12.13\pm0.75\pm0.44$
0.25	$4.69\pm0.14\pm0.36$	$4.58\pm0.24\pm0.02$	$4.37\pm0.46\pm0.34$
0.35	$1.89\pm0.09\pm0.02$	$1.99\pm0.17\pm0.16$	$2.19\pm0.31\pm0.17$
0.45	$0.78\pm0.06\pm0.01$	$1.02\pm0.12\pm0.03$	$1.51\pm0.22\pm0.04$
0.55	$0.37\pm0.04\pm0.01$	$0.24\pm0.05\pm0.02$	$-0.01\pm0.11\pm0.01$
0.65	$0.15\pm0.02\pm0.01$	$0.19\pm0.05\pm0.02$	$0.26\pm0.10\pm0.02$
0.75	$0.07\pm0.02\pm0.01$	$0.06\pm0.03\pm0.01$	$0.05\pm0.05\pm0.01$

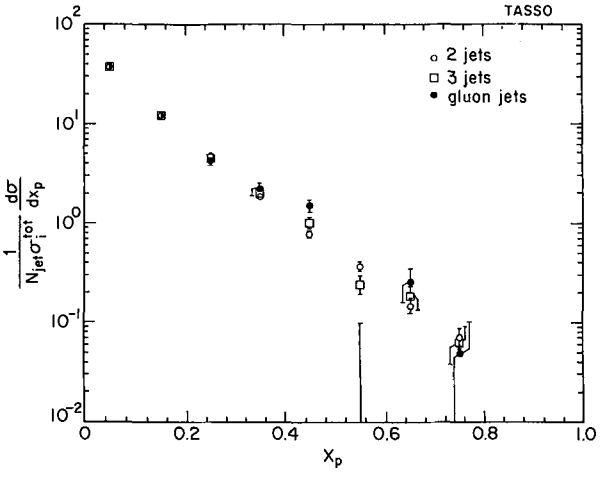

Fig. 2. Inclusive $d\sigma/dx_p$ distributions for 2-jet events, symmetric 3-jet events and gluon jets. N_{jet} is 2, 3 and 1 for 2-jet, 3-jet and gluon jet, respectively. σ_i^{tot} is the total cross section for our 2-jet ($i=2$) and 3-jet or gluon jet ($i=3$) sample. The errors are statistical only

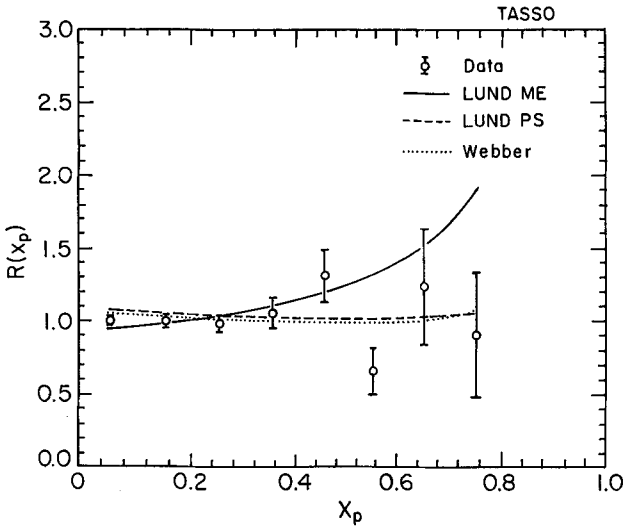

Fig. 3. $R(x_p)$, as defined in Sect. 3, for: data; LUND Monte Carlo with second order matrix element in α_s (ME); LUND Monte Carlo with parton shower (PS); Webber Monte Carlo. The errors are statistical only

Another way to present the data is to calculate the following ratio [5]:

$$R(x_p)=\frac{\frac{1}{3\sigma_3^{\text{tot}}}\frac{d\sigma}{dx_p}(\text{3-jets})}{\frac{1}{2\sigma_2^{\text{tot}}}\frac{d\sigma}{dx_p}(\text{2-jets})}$$

which is shown in Fig. 3. We plot also the same $R(x_p)$ for 3 Monte Carlo models: the LUND model [13] with matrix elements calculated up to second order in α_s (ME), the LUND model [13] with parton shower (PS) and the Webber model [23], which is a parton shower model. All the Monte Carlo curves were calculated with parameters tuned to the 35 GeV data. As indicated by MARK II [5], $R(x)$ may be less sensitive to changes in parameters of the various models, since they are common to the 3-jet and 2-jet samples, and by taking their ratio, the uncertainties in some features of the models should be reduced.

We can see from Fig. 3 that $R(x_p)$ is nearly flat in x_p and is described correctly both by the Webber Monte Carlo and by the LUND Monte Carlo with the parton shower option, while the LUND model with second order in α_s predicts an increase at high x_p. This effect is mainly due to a softer x_p distribution in the events generated at 22 GeV. We varied the parameters which are more sensitive to the x_p distributions over a wide range of values for both LUND Monte Carlo simulations and compared the results with the 35 GeV and 22 GeV inclusive x_p distributions. The parameters tuned to the 35 GeV data described well the 22 GeV data for the parton shower

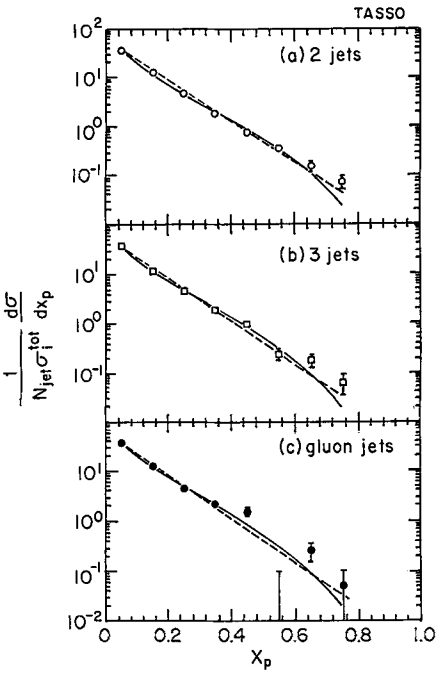

Fig. 4a–c. Inclusive $d\sigma/dx_p$ distributions of data together with fits to the functions $f(x_p)$ (solid line) and $g(x_p)$ (dashed line) defined in Sect. 3. N_{jet} and σ_i^{tot} are as in Fig. 2. The errors include both statistical and systematic uncertainties, added in quadrature. **a** 2-jet events, **b** 3-jet events, **c** Extracted gluon jets

model, while the finite order α_s model could not describe well the 22 GeV data with the same parameters. A similar disagreement in the ratio of inclusive x_p distributions at different energies between the data and a LUND finite order model has been reported by JADE [24].

We also checked the variation of $R(x_p)$ with the model parameters. $R(x_p)$ changes slowly with the parameters, the variation being larger for high x_p. It is typically of the order of a few percent up to $x_p \sim 0.3$ for both LUND models. For the parton shower model it is less than 15% up to $x_p \sim 0.75$, and of the order of 40% for $x_p=0.8$. For the finite order α_s model it is less than 15% up to $x_p \sim 0.6$, of the order of 30% for $0.6<x_p<0.75$ and of the order of 50% for $x_p=0.8$. The variation covers a large range of the parameters. For high x_p values, $R(x_p)$ for the finite order α_s model lies above $R(x_p)$ for the parton shower model, for most parameter sets used.

The x_p distributions of Fig. 2 were fitted to the function:

$$f(x_p)=\frac{A}{x_p^a}(1-x_p)^b$$

where A is a normalization constant and a and b are arbitrary parameters. For the fit, x_p is taken at

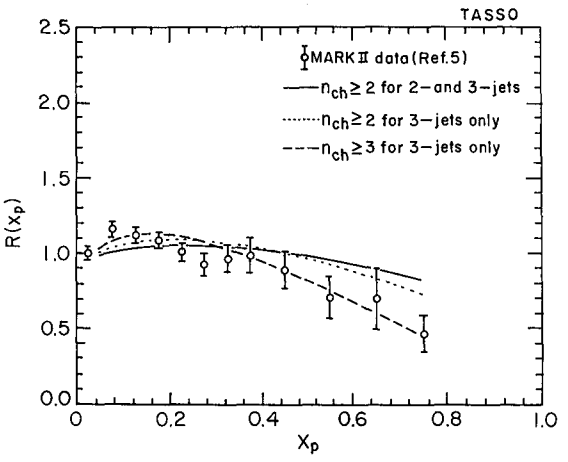

Fig. 5. Comparison of $R(x_p)$ distributions between MARK II [5] (data points) and our data (curves). The ratio $R(x_p)$ in the curves is calculated from the 2-jet and 3-jet x_p distributions, including systematic errors, fitted to the function $f(x_p)$ with different charge multiplicity (n_{ch}) cuts. The solid line corresponds to the cuts used in this work, i.e. at least 2 charged particles per jet for the 2-jet and 3-jet samples. The dotted (dashed) line corresponds to a cut of at least 2 (3) charged particles per jet for the 3-jet sample only

the centre of each bin. This form is an approximation of the most general function [25] that describes fragmentation of a string system in a symmetric way with respect to both string ends, omitting the dependence on the transverse mass of a hadron. Systematic errors, estimated in Sect. 2.4, were included in the fits. Other functional forms, such as exponentials and polynomials, were also applied to fit these x_p distributions. In Fig. 4 we show for 2-jet events, 3-jet events and the extracted gluon jet, the data and fits to the function $f(x_p)$ (solid curve) and to an exponential function of the form $g(x_p) = Ce^{-\alpha x_p}$ (dashed curve). The numerical values of the free parameters a and b in the fit to $f(x_p)$ lie in the range $0.6 < a < 0.7$ and $4.2 < b < 4.5$ for all three fits with errors of 10–15%. The parameter α in the exponential fits lies between 9.6 and 10.0 with errors below 4%. All curves represent the trend of the data quite well, and the χ^2/DOF values of these fits vary between 2 and 4.

To compare our result with MARK II [5], we repeated the analysis by applying jet multiplicity cuts on the 3-jet data with no similar cuts on the 2-jet data for 2 different conditions: a) at least 2 charged particles in each jet; b) at least 3 charged particles in each jet. These cuts are an approximation of the cuts in [5], where they demand that each jet in the 3-jet events has a total (charged plus neutral) multiplicity of at least 3. The results are presented in Fig. 5, where the MARK II data points are shown together with our $R(x_p)$ distributions calculated with various multiplicity cuts from the 2-jet and 3-jet x_p distributions, fitted to the function $f(x_p)$ defined above. The solid curve is calculated with the cuts used in this work, and is thus equal to the ratio of the solid curves of Fig. 4b and a. The dotted (dashed) curve has a cut of at least 2 (3) on the jet multiplicity in the 3-jet events. The statistical significance of the difference between the solid and dashed curves in the region $x_p > 0.4$ is of the order of one standard deviation for each measured point (0.1 x_p bins). The trend of the curves shows that for larger multiplicity cuts, $R(x_p)$ falls more rapidly with x_p.

The $R(x_p)$ distributions were also calculated with the same multiplicity cuts, replacing the $f(x_p)$ function by $g(x_p)$. A similar trend concerning the $R(x_p)$ fall-off is obtained (not shown), but the effect is less significant. Alternatively, the ratio $R(x_p)$ calculated directly from the data, as in Fig. 3, has been fitted for the various multiplicity cuts to an exponential function and to a linear function. Both functions give essentially identifical fits with χ^2/DOF values between 1.2 and 1.3. For the linear form $R(x_p) = B - Dx_p$ and multiplicity cuts as used in this paper, the fit is consistent with a flat distribution, yielding $D = 0.06 \pm 0.23$. Requiring at least 3 charged particles only for the 3-jet sample yields $D = 0.49 \pm 0.21$, indicating a decreasing function as obtained also for the previous fits. We conclude that selective multiplicity cuts only on 3-jet events tend to produce a faster decrease in $R(x_p)$ with x_p, which was interpreted as a softer fragmentation for gluon jets [5].

4 Discussion and conclusions

We do not observe any significant difference between the fragmentation of a gluon jet and that of a quark jet, both of ~ 11 GeV jet energies. Most of the results in e^+e^- annihilation at PETRA-PEP energies are consistent with this statement, for example the ratio of gluon and quark jet multiplicities, as given in [4], is consistent with one. At higher energies, the results of UA1 [9] for jets with transverse momentum up to 40 GeV indicate a difference between the two types of jets. These results, combined with the theoretical predictions [2] that the differences in multiplicity between quark and gluon jets grow with energy, suggest that higher energy hadron colliders, as well as LEP-SLC, will have a better chance to find differences between quark and gluon fragmentation.

The extraction of the gluon x_p distribution in the MARK II analysis [5] uses as a 2-jet sample an interpolation of inclusive data from other experiments. Therefore, they could not apply any cuts on their 2-jet sample. The softer gluon fragmentation that they obtain may originate from the cuts on jet multiplicity, applied on their 3-jet symmetric sample, but not on the 2-jet one. As shown in Fig. 5, increasing the cut

on the minimum number of particles in the 3-jet sample, with no similar cut for the 2-jet events, produces an apparent softening in the gluon jet distribution. This effect is also observed in Monte Carlo simulation.

Recently the AMY Collaboration [26] at TRISTAN, using uncorrected data, has reported a significant difference in the rapidity of the leading particle between the two fastest jets and the slowest jet in their 3-jet sample. However, the value of rapidity for leading particles with high longitudinal momentum is strongly dependent on the jet axis determination [11]. Therefore, a comparison of the rapidity of a leading particle in our 2-jet and 3-jet data sets is not meaningful, since the jet algorithm used in the 3-jet sample cannot be applied on the 2-jet sample. Moreover, a gluon jet in non-symmetric 3-jet events is more likely to be the least energetic jet, predictions for the probability of which are model dependent.

As an additional check we have measured the uncorrected mean rapidities of leading particles in our inclusive non-symmetric 3-jet sample of 5830 events with $\bar{W} = 34.8$ GeV. The jet energies were reconstructed from the angles between the jets and the jets were then ordered in energy, such that jet 3 is the least energetic one. The mean rapidity of the leading particle was calculated in each jet as a function of the jet energy. No significant differences were found for the rapidities of jet 2 (mainly quark) and jet 3 (mainly gluon), for the same jet energies. For a 10 GeV jet, the mean uncorrected rapidity of the leading particle for jet 2 is 2.76 ± 0.04 and for jet 3 we obtain 2.63 ± 0.04. The errors on the mean values are statistical only.

Concerning the Monte Carlo simulation models, we find that models based on parton showers describe the trend of the data better than a finite order model with a second order matrix element in α_s. Note that the two options of the LUND Monte Carlo, the parton shower and the matrix element, use the same fragmentation scheme. The sensitivity of the ratio $R(x_p)$, defined in the previous section, to changes in the model parameters is larger in the matrix element scheme, compared to the parton shower one.

We have checked how well the two versions of the LUND Monte Carlo describe the x_p distribution at $W = 22$ GeV, using the parameters tuned for the $W = 35$ GeV sample. The parton shower model describes the data quite well, while the matrix element model tends to soften the x_p distribution with these parameters. This is probably due to the fact that models with parton shower start the fragmentation process when the virtuality of the partons is low (typically of the order of 1 GeV), so the main characteristics of an event are given by the parton cascade, and the role of fragmentation is diminished. One way to cure this problem of the α_s^2 matrix element model is to include explicitly an energy dependence in the parameters of the fragmentation function [24]. The trend of the energy dependence suggested by [24] is consistent with the softening of the 22 GeV x_p distribution. Alternatively, reasonable results can be obtained with different parameter tuning to the data at each energy. However, as noted before [21, 27], it is preferable to use parton shower models to study e^+e^- events at high energies where no data are yet available.

In summary, we have extracted the gluon x_p distribution by comparing 3-jet symmetric events at $W \sim 35$ GeV with 2-jet events at $W \sim 22$ GeV. We do not observe a difference in the x_p distribution of quark and gluon jets. The method used is almost independent of the jet axis determination and does not rely on models that determine which jet is the gluon jet. This result does not confirm the MARK II measurement [5]. The difference may be due to inconsistent multiplicity cuts, as discussed above. More statistics and higher energies are probably needed for the confirmation of the predicted differences between quark and gluon fragmentation.

Acknowledgements. We gratefully acknowledge the support by the DESY directorate, the PETRA machine group and the DESY computer centre. Those of us from outside DESY wish to thank the DESY directorate for the hospitality extended to us while working at DESY.

References

1. S.J. Brodsky, J. Gunion: Phys. Rev. Lett. 37 (1976) 402; A. Bassetto, M. Ciafaloni, G. Marchesini: Nucl. Phys. B163 (1980) 477
2. G.Sh. Dzhaparidze, Z. Phys. C – Particles and Fields 32 (1986) 59; G.Sh. Dzhaparidze: IHEP Preprint 86–100, Sepurkhov (1986)
3. A.H. Mueller: Nucl. Phys. B241 (1984) 141; A.H. Mueller: J.B. Gaffney, Nucl. Phys. B250 (1985) 109
4. HRS Coll., M. Derrick et al.: Phys. Lett. 165B (1985) 449; K. Sugano: Int. J. Mod. Phys. A3 (1988) 2249
5. MARK II Coll., A. Petersen et al.: Phys. Rev. Lett. 55 (1985) 1954
6. JADE Coll., W. Bartel et al.: Phys. Lett. 123B (1983) 460
7. TPC Coll., R.J. Madaras: Rencontre de Moriond on Strong Interaction and Gauge Theories, Les Arcs (1986)
8. CELLO Coll.: Contributed paper to the International Symposium on Lepton and Photon Interactions at High Energies, Hamburg, 1987
9. UA1 Coll., G. Arnison et al.: Nucl. Phys. B276 (1986) 253
10. TASSO Coll., R. Brandelik et al.: Phys. Lett. B83 (1979) 261; TASSO Coll., R. Brandelik et al.: Z. Phys. C – Particles and Fields 4 (1980) 87
11. TASSO Coll., M. Althoff et al.: Z. Phys. C – Particles and Fields 22 (1984) 307
12. TASSO Coll., W. Braunschweig et al.: DESY 88-107 preprint, 1988, and Z. Phys. C (to be published); P. Dauncey: Oxford D. Phil. Thesis, RAL T 034 (1986)

13. T. Sjöstrand: Comput. Phys. Commun. 39 (1986) 347; T. Sjöstrand, M. Bengtsson: Comput. Phys. Commun. 43 (1987) 367
14. Weizmann Inst. Group: TASSO Monte Carlo Programm (MONSTER), TASSO Notes 40, 60 and 89 (unpublished)
15. H. Daum, H. Meyer, J. Bürger: Z. Phys. C – Particles and Fields 8 (1981) 167
16. JADE Coll., W. Bartel et al.: Z. Phys. C – Particles and Fields 33 (1986) 23
17. S.L. Wu, G. Zobernig: Z. Phys. C – Particles and Fields 2 (1979) 107
18. G. Sterman, S. Weinberg: Phys. Rev. Lett. 39 (1977) 1436; K. Fabricius, I. Schmitt, G. Kramer, G. Schierholz: Z. Phys. C – Particles and Fields 11 (1981) 315
19. F. Gutbrod, G. Kramer, G. Schierholz: Z. Phys. C – Particles and Fields 21 (1984) 235
20. TASSO Coll., M. Althoff et al.: Z. Phys. C – Particles and Fields 29 (1985) 29
21. TASSO Coll., W. Braunschweig et al.: Phys. Lett. B214 (1988) 286
22. G. Kramer, B. Lampe: Z. Phys. C – Particles and Fields 39 (1988) 101
23. G. Marchesini, B.R. Webber: Nucl. Phys. B238 (1984) 1; B.R. Webber: Nucl. Phys. B238 (1984) 492
24. JADE Coll., W. Bartel et al.: Z. Phys. C – Particles and Fields 20 (1983) 187
25. B. Andersson, G. Gustafson, B. Söderberg, Z. Phys. C – Particles and Fields 20 (1983) 317
26. S.L. Olsen AMY Coll.: ER-13065-556 preprint, presented at the XXIV International Conference on High Energy Physics, München 1988
27. MARK II Coll., A. Petersen et al.: Phys. Rev. D37 (1988) 1